Sadeghi *et al. Biochar* (2026) 8:35
https://doi.org/10.1007/s42773-025-00505-8

Biochar

ORIGINAL RESEARCH Open Access

Introducing priority morph-genetic porous carbon for potential applications in soil and water conservation through game theory

Seyed Hamidreza Sadeghi[1,2*], Somayeh Zare[1], Sudabeh Gharehmahmudli[1], Habibollah Younesi[3], Fengbao Zhang[4], Mahboubeh Mirzahosseini[1], Padideh Sadat Sadeghi[1], Mehdi Homaee[1,5], Yahya Parvizi[6], Shen Nan[7] and Yao Li[8]

Abstract

The increasing generation of solid waste is recognized as one of the leading environmental and economic challenges. Optimal waste management, particularly in the agricultural and industrial sectors, necessitates innovative approaches for the efficient management of vital resources, including soil and water. One practical solution is the production of morpho-genetic porous carbon (MGPC) as a type of activated biochar, which has wide applications due to its porous structure, chemical and thermal stability, and high specific surface area. In this study, biochar was prepared with eight types of waste, including rice straw, vineyard prunings, palm prunings, sawdust, vinasse, poultry slaughterhouse waste, paper mill waste, and tissue paper production waste. Biochar production was carried out through a pyrolysis process under low-oxygen conditions and at a temperature of 400 °C. Biochar was converted into MGPC at a temperature of 800 °C using KOH and H_3PO_4 as activators at three different levels and CO_2 at a single level. Then, using data obtained from the Brunauer–Emmet–Teller (BET) test, the game theory approach, and the Condorcet algorithm for evaluation, 64 MGPC samples were analyzed. BET analysis was performed to measure the specific surface area and pore structure. The data obtained from this analysis were extensively reported, encompassing approximately 40 criteria. However, only 12 criteria were selected, while about 28 criteria were excluded from the Condorcet algorithm due to the incompleteness of some of their data. This study investigated the process of biochar and MGPC production using agricultural and industrial wastes, with an emphasis on the role of game theory in promoting environmentally sound decision-making and optimizing MGPC applications. From 64 prepared samples, by examining their physical properties and environmental impacts, five priority samples, i.e., rice straw-KOH-level 2, sawdust-KOH-level 2, palm tree pruning waste-KOH-level 2, vineyard pruning waste-KOH-level 2, and tissue factory waste-KOH-level 2, with respective surface areas of 1071.47, 672.04, 860.54, 667.49, and 133.45 $m^2\ g^{-1}$ and t-plot micropore volumes of 0.29, 0.24, 0.17, 0.19, and 0.02 $cm^3\ g^{-1}$. were prioritized using the Condorcet algorithm. They were identified as suitable candidates for advanced applications in soil and water conservation due to their favorable porous structures and highly performed BET properties. The present study shows that innovative methods for producing MGPC can improve the performance and properties of porous materials for various applications.

*Correspondence:
Seyed Hamidreza Sadeghi
sadeghi@modares.ac.ir
Full list of author information is available at the end of the article

Springer

Highlights

- Problematic wastes can be managed by producing morph-genetic porous carbon (MGPC).
- 64 MGPCs were produced from different agricultural and industrial wastes.
- Priority MGPC was introduced to revolutionize soil and water conservation.
- Five better-performed MGPCs were classified using game theory.
- 1:2-KOH-activated rice straw MGPC performed better for soil and water conservation.

Keywords Activated carbon, Multi-criteria decision making, Physical properties, Soil amendment, Waste management

Graphical Abstract

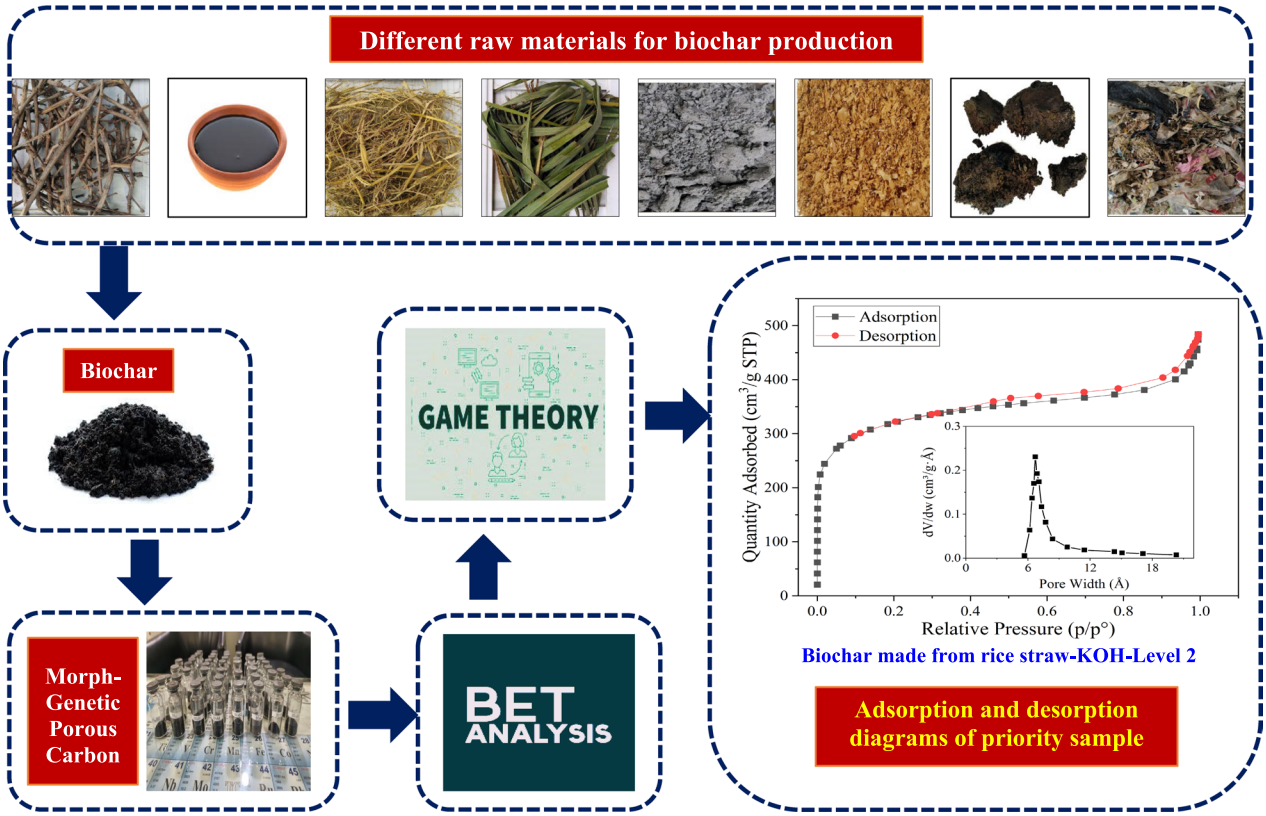

1 Introduction

The biosphere cannot exist without soil, which is a crucial component of both natural and anthropogenic ecosystems (Amundson et al. 2015). Nevertheless, land degradation and soil erosion pose a serious threat to food security, access to water, and the stability of the Earth system. Approximately 75% of the world's land has already been degraded, and 24 billion tons of soil are eroded annually (FAO 2021; Montanarella et al. 2023). Agricultural and environmental crises are exacerbated by the projection that 90 percent of the land could be degraded by 2050 unless better practices are implemented (Pimentel 2020).

The global trend toward industrialization, combined with expectations of a better quality of life and social welfare, has led to the production of a large amount of solid waste (Bhagawan et al. 2017). Simultaneously, with the processes of industrialization and urbanization,

more than three billion tons of solid waste are produced annually (Voukkali et al. 2024), which can be divided into municipal, medical, hazardous, agricultural, and industrial (Galab et al. 2004; Gehrlein and Fishburn 2023; Tideman 2023; Black 2025; Riker 2025). As in the case of the Middle East, inefficiencies in waste management are also evident, with limitations primarily in collection and disposal due to poor infrastructure and inadequate funding (Hemidat et al. 2022).

Waste management is one of the fundamental requirements of any society, considering the difficulties and problems associated with it (Zohoori and Ghani 2017). Strategies such as recycling waste into valuable products, including biochar, are essential for reducing adverse environmental effects (Smith et al. 2025). Biochar, a carbon-rich substance produced by the pyrolysis of organic waste, enhances soil fertility and improves water retention (Bahrami et al. 2018; Hewitt et al. 2023). It has proven effective in various environments for soil and water conservation (Sadeghi et al. 2016, 2018, 2020). Nevertheless, when compared with traditional biochar, activated carbon, especially Morph-Genetic Porous Carbon (MGPC), demonstrates better capabilities in numerous applications because it has an increased porosity and surface area (Park et al. 2025). The formation of MGPC occurs through chemical (KOH, H_3PO_4) or physical (CO_2) activation, thereby developing materials with higher adsorption capacity and stability (Li et al. 2025; Wang et al. 2023, 2025a, b). Such characteristics ensure that MGPC is an excellent choice for removing pollutants, improving soil adsorption, and storing energy (Kim et al. 2025).

Because biochar is considered a highly developed material with a wide range of applications in environmental and industrial spheres, there is a need for in-depth studies of application requirements and detailed reviews of its properties to enable the optimal selection of biochar, which is produced under different conditions and by various processes. Optimal production conditions can be created using appropriate raw materials and structural modifications to produce high-performance samples specific to soil and water conservation (Sadeghi et al. 2021; Zhou et al. 2025). Not only does this economic process enhance economic efficiency, but it also has a positive impact on the environment (Li et al. 2023a, b; Wang et al. 2025a, b). Evaluating the best MGPC samples requires an effective multi-criteria decision-making (MCDM) methodology. MCDM approaches based on traditional methods are usually sensitive and vulnerable due to conflicts in weighting and data (Saaty 1980; Roy 1996). In recent years, MCDM has emerged as a crucial tool for managing complex environmental and materials engineering problems. However, conventional MCDM methods face challenges such as high sensitivity to criterion weighting and difficulties in handling of data conflicts and ambiguities, which can lead to unstable and inconsistent results (Saaty 1980; Roy 1996; Adhami et al. 2020; Chen et al. 2023a, b). Convincingly, game theory and its Condorcet algorithm propose a more dynamic approach, as they rank alternatives using pairwise comparisons and minimize dependency on subjective weightings (Avand et al. 2023; Sadeghi et al. 2024). The Condorcet algorithm, based on game theory and paired comparisons, is a practical and easy-to-use method in multi-criteria decision-making, which has significantly reduced these challenges. By focusing on selecting the option that offers the most significant advantage in paired comparisons, this algorithm reduces dependence on precise weighting and sensitivity to changes in weights, making the decision-making process interactive and dynamic (Avand et al. 2023). The approach has been effectively applied in biochar studies to find a balance between environmental, economic, and technical requirements (Lee et al. 2022a, b; Chen et al. 2023a, b). The Condorcet algorithm has also been employed to determine the environmental sustainability of biochar optimally (Smith et al. 2022), enhance soil amendment and agricultural efficiency, and address climate change (Brown et al. 2024). The proposed approach yields more cost-effective and eco-friendly decisions (Zhang and Li 2020; Perea and Grima 2021), as well as plans for reaching a common agreement within the biochar supply chain (Wang et al. 2023; Zhang et al. 2024a, b). Kumar et al. (2025a, b) employed game theory to model the dynamic impact of changes in the preference criteria for biochar selection, taking into account both economic and environmental factors. Recently, Martinez et al. (2025) focused on the development of biochar technologies and applied the Condorcet method to the multi-criteria assessment and prioritization of variations in biochar usage. This study concluded that the Condorcet method can be characterized as successful in identifying the best biochar technologies and in guiding the ranking of appropriate solutions for various applications. This algorithm determines the alternatives that are most successful in comparison with others (Nasiri Khiavi et al. 2024).

It has been found that biochar production and utilization as a novel method in biowaste recycling can promote sustainable farming growth and natural resource preservation. Nevertheless, the comparative analyses suggest that the application of decision-making tools, such as game theory, in biochar selection and prioritization leads to optimal and sustainable decision-making in biochar-related contexts. The inclusion of

the Condorcet algorithm in Brunauer–Emmett–Teller (BET) analysis, an experimentally validated method for measuring the properties of porous materials, is also explored in this study (Zhu et al. 2023). The MCDM gaps can be overcome by using BET-based metrics (e.g., surface area, pore volume) as objective inputs in MGPC. This approach enables the science-based prioritization of MGPC samples, making it reproducible and instrumental in arid and semi-arid regions that face water scarcity, soil salinization, and reduced fertility (Khan et al. 2023). Countries like Iran and other Middle Eastern nations, which face harsh climatic conditions and require soil improvement and sustainable water resource management, will benefit the most from this approach. MGPC, as a sustainable and practical material for improving the physical, chemical, and biological properties of soil, can play a key role in increasing agricultural yields and preserving the environment, especially in these regions.

Three main contributions distinguish the current research: (1) It introduces a novel framework that integrates game theory (i.e., Condorcet algorithm) and BET to precisely and objectively prioritize Morph-Genetic Porous Carbon (MGPC)—a biochar alternative designed to overcome subjective prioritization among incompatible or conflicting properties of biochars; (2) The research employs waste valorization, converting a wide range of agricultural and industrial wastes (e.g., rice straw, sawdust) into high-performance MGPC; (3) It holds potential for sustainable resource management by bridging the gap between the highly advanced decision-making analysis and material science, thereby establishing a reproducible model for future applications.

2 Materials and methods

The present study aimed to investigate and analyze the use of game theory decision-making tools in the selection and prioritization of morph-genetic porous carbon produced from agricultural and industrial wastes for use in soil and water conservation. In this study, agricultural and industrial wastes, including rice straw, vineyard pruning, palm pruning, sawdust, vinasse, poultry slaughterhouse waste, paper mill waste, and tissue paper production waste, were selected and collected to produce biochar. Then, after preparing biochar at a temperature of about 400 °C, genetically modified porous carbon was produced by physical (CO_2) and chemical (H_3PO_4, KOH) activation methods with different ratios of 1:1, 1:2 and 1:3. Finally, game theory was used to select optimal samples for conducting experiments related to soil and water conservation. In this research, the Condorcet algorithm was employed within the framework of game theory to prioritize and optimally select 62 genetically modified porous carbon samples produced from various biological sources. The associated flowchart for the multiple steps of the research is shown in Fig. 1.

2.1 Waste selection and raw material preparation

The preparation of raw materials for biochar and MGPC production is a multi-stage and sensitive process that requires the precise selection of raw materials, optimal preparation, and appropriate structural processing. In the initial stage, comprehensive data on waste generation sources were collected. This information included the physical and chemical characteristics of the waste, as well as its production volume and type. In this phase, the environmental impacts of each waste type, including pollution potential and environmental hazards, were also analyzed. Subsequently, samples of interest were prepared, including rice straw and husk residues, vineyard pruning residue, palm pruning residue, sawdust, vinasse, poultry slaughterhouse waste, paper mill waste, and tissue production residues. A general view of the selected raw materials is shown in Fig. 2.

2.2 Production of Biochar

Biochar is a valuable environmental product produced through thermally controlled processes using biomass resources such as agricultural residues and industrial biowastes (Kumar et al. 2025a, b). This process involves several basic steps that are carried out continuously and optimally to produce a high-quality product with suitable performance for various applications. The raw materials were prepared from rice field waste, vineyard and palm tree pruning waste, sugarcane industry waste (vinasse), poultry slaughterhouse waste, paper factory waste, tissue paper factory waste, and sawdust from the wood industry. After preparation, the raw materials were dried and chopped into pieces. Then, the dried and ground materials were pyrolyzed at 400 °C in an oxygen-free environment. The time required for pyrolysis varied depending on the moisture content and type of raw material (Li et al. 2025). The initial samples were ground to particles with a size between 1 and 2 mm after complete drying at 105 °C for 24 h. In the next stage, the pyrolysis operation was conducted in a horizontal tubular reactor under a continuous flow of pure nitrogen at a rate of 150 mL min^{-1}. The temperature increased at a rate of 10 °C min^{-1} until it reached the target temperature of approximately 400 °C. The material was maintained at this thermal condition for about four hours to complete the pyrolysis process.

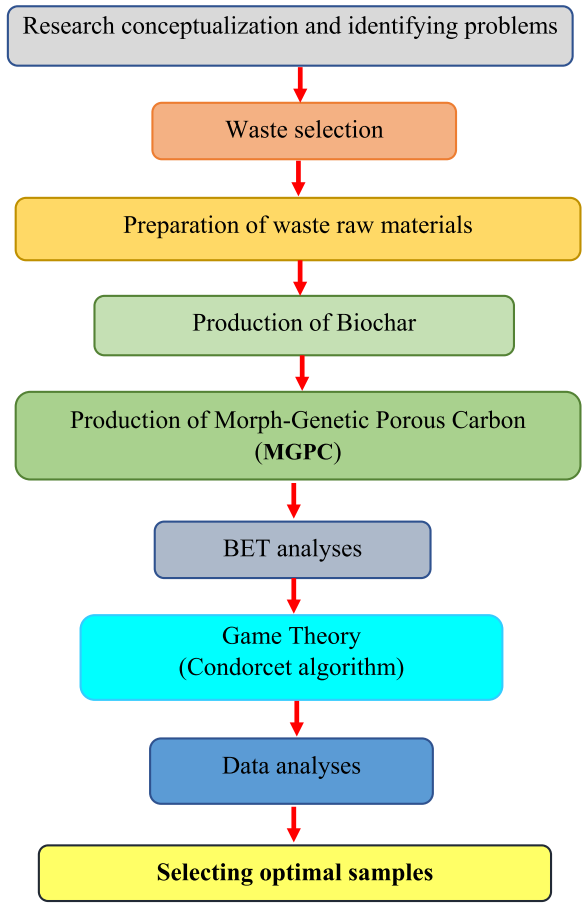

Fig. 1 Flowchart and research implementation steps

2.3 Production of Morph-Genetic Porous Carbon (MGPC)

MGPC was produced from the initial biochar as the base material and included several structural and chemical modification steps to optimize its properties for specific applications (Li et al. 2023a, b). This porous, carbon-rich, and fine-grained material was produced at a temperature of about 800 °C in an oxygen-free environment. The production process included two primary physical and chemical activation methods. In the chemical method, the activating agents, KOH and H_3PO_4, were used on the initial biochar samples in 1:1, 1:2, and 1:3 ratios. For this purpose, five grams of biochar were mixed with proportional amounts of 5, 10, and 15 g of KOH or H_3PO_4, respectively, along with distilled water, until the mixture was diluted. The mixture was then dried at 105 °C for 24–72 h. Subsequently, the samples were subjected to thermal decomposition in an oven under argon gas flow at high temperatures for about 5–8 h (Wang et al. 2023; Kumar et al. 2025a, b). For physical activation, the initial biochar was subjected to thermal decomposition in the presence of CO_2 at high temperatures. CO_2 was injected at a rate of 200 mL min^{-1} to increase the porosity of the structure through direct reaction with carbon, which is highly effective in enhancing the thermal stability of the material. The selection of these three activators was made to compare the performance of different methods, and they were evaluated in terms of efficiency, environmental compatibility, and impact on the structural properties of the samples. The samples were eventually washed repeatedly with distilled water to neutralize their pH. If

Fig. 2 Raw materials for biochar production, including 1) Vineyard pruning waste, 2) Vinasse, 3) Rice straw, 4) Vineyard pruning waste, 5) Tissue paper factory waste, 6) Sawdust, 7) Poultry slaughtering waste cake, and 8) Paper factory waste

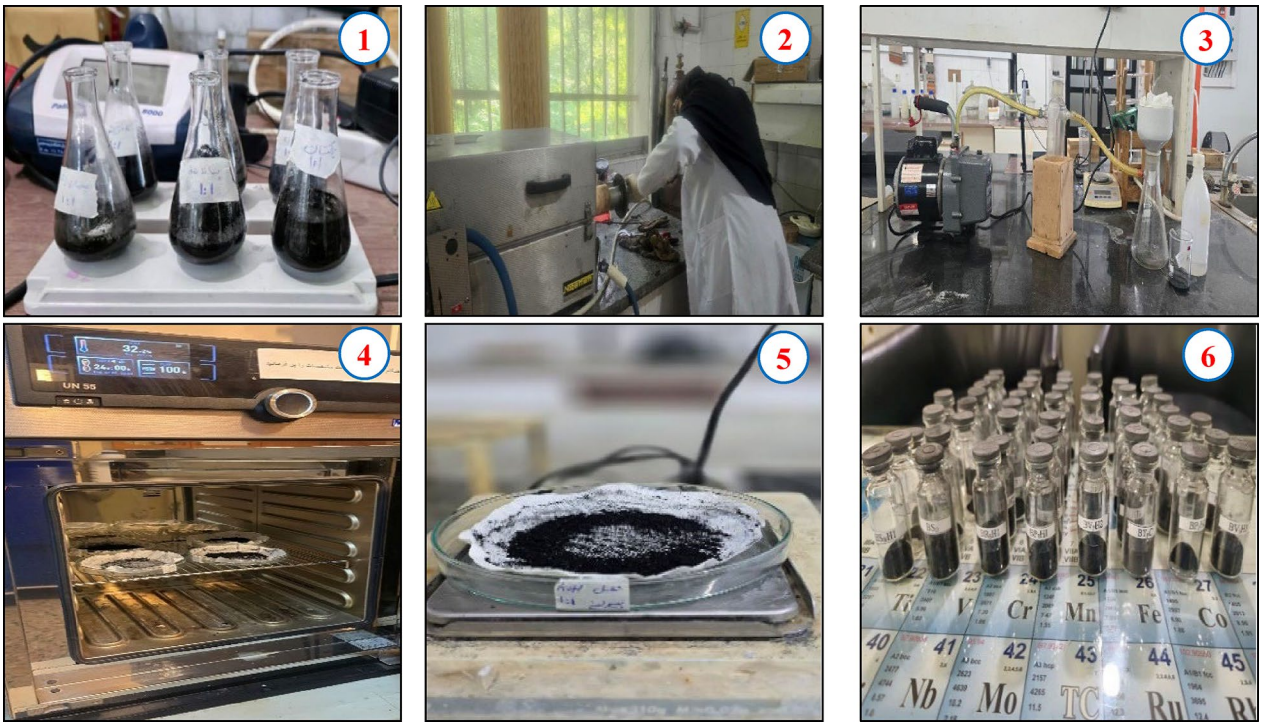

Fig. 3 Steps for preparing Morph-Genetic Porous Carbon (MGPC) from biochar, including 1) Diluting with distilled water, mixing and drying five grams of biochar with appropriate amounts of KOH or H_3PO_4, 2) Injecting argon gas in a furnace at a temperature of about 800 °C for some 5 to 8 h, 3) Washing samples with distilled water and adjusting pH with nitric acid or sodium hydroxide solutions, 4) Drying the final samples in the oven, 5) Weighing the final samples, and 6) Sending prepared samples for BET analysis

necessary, pH adjustments were performed by washing with dilute nitric acid or sodium hydroxide solutions, and the samples were then dried at 105 °C. This step was usually performed empirically using a trial-and-error approach (Zhang et al. 2024a, b). Ultimately, the final samples were weighed after washing and drying in an oven and prepared for visual and BET tests. The different stages and the entire list of products are illustrated in Fig. 3 and summarized in Table 1. The visual test was performed based on the color of the product. The blacker the color, the higher the carbon content. Gray products that indicated ash were removed from the above list.

2.4 Application of BET analysis

To assess the suitability of the produced MGPCs for soil and water conservation, BET analysis was employed as a physical method for measuring the specific surface area and porosity of solid materials. This method is based on the adsorption of gas molecules (commonly nitrogen) onto the material's surface at a temperature of liquid nitrogen (77 K). By gradually increasing the gas pressure, the amount of gas adsorbed by the material is measured, followed by desorption as the pressure decreases. The results are presented as adsorption and desorption isotherms, from which essential factors, including specific surface area, pore volume, and pore size distribution, can be derived. BET analysis is widely used in studying materials such as catalysts, nano-adsorbents, composites, additives, pharmaceuticals, and nanostructures (e.g., metal nanoparticles, nanotubes, and nanofibers). Overall, BET analysis is a powerful tool for investigating the surface characteristics of porous materials and plays a significant role in developing and enhancing material performance across various applications. For BET analysis in this study, all samples were prepared according to laboratory protocols and securely packaged for delivery to the designated laboratory.

2.5 Application of game theory

Since some parameters of the produced MGPCs are conflicting, decision-making on the priority production needs robust MCDM approaches (Roy et al. 2023). Accordingly, one of the most widely applied and easiest game theory approaches. i.e., the Condorcet algorithm was applied to help comprehensively select the top-most MGPCs. The Condorcet algorithm, named after the French mathematician Marie Jean Antoine Nicolas de Caritat, Marquis de Condorcet, is a group decision-making method used to identify a winning option

Table 1 Details on preparation of Morph-Genetic Porous Carbon (MGPC)

No.	Biochar source	Temperature for biochar	Activator	Rate	Symbol	Temperature for MGPC
1	Rice straw (BR_S)	400 °C	KOH	1:1	BR_SK1	800 °C
				1:2	BR_SK2	
				1:3	BR_SK3	
			H_3PO_4	1:1	BR_SH1	
				1:2	BR_SH2	
				1:3	BR_SH3	
			CO_2	–	BR_SC	
2	Vineyard pruning waste (BV_P)	400 °C	KOH	1:1	BV_PK1	800 °C
				1:2	BV_PK2	
				1:3	BV_PK3	
			H_3PO_4	1:1	BV_PH1	
				1:2	BV_PH2	
				1:3	BV_PH3	
			CO_2	–	BV_PC	
3	Palm tree pruning waste (BP_T)	400 °C	KOH	1:1	BP_TK1	800 °C
				1:2	BP_TK2	
				1:3	BP_TK3	
			H_3PO_4	1:1	BP_TH1	
				1:2	BP_TH2	
				1:3	BP_TH3	
			CO_2	–	BP_TC	
4	Sawdust (BS_D)	400 °C	KOH	1:1	BS_DK1	800 °C
				1:2	BS_DK2	
				1:3	BS_DK3	
			H_3PO_4	1:1	BS_DH1	
				1:2	BS_DH2	
				1:3	BS_DH3	
			CO_2	–	BS_DC	
5	Poultry slaughtering waste cake (BS_W)	400 °C	KOH	1:1	BS_WK1	800 °C
				1:2	BS_WK2	
				1:3	BS_WK3	
			H_3PO_4	1:1	BS_WH1	
				1:2	BS_WH2	
				1:3	BS_WH3	
			CO_2	–	BS_WC	
6	Paper factory waste (BP_F)	400 °C	KOH	1:1	BP_FK1	800 °C
				1:2	BP_FK2	
				1:3	BP_FK3	
			H_3PO_4	1:1	BP_FH1	
				1:2	BP_FH2	
				1:3	BP_FH3	
			CO_2	–	BP_FC	
7	Tissue paper factory waste (BT_P)	400 °C	KOH	1:1	BT_PK1	800 °C
				1:2	BT_PK2	
				1:3	BT_PK3	
			H_3PO_4	1:1	BT_PH1	
				1:2	BT_PH2	
				1:3	BT_PH3	
			CO_2	–	BT_PC	

Table 1 (continued)

No.	Biochar source	Temperature for biochar	Activator	Rate	Symbol	Temperature for MGPC
8	Vinasse (BV_I)	400 °C	KOH	1:1	BV_IK1	800 °C
				1:2	BV_IK2	
				1:3	BV_IK3	
			H_3PO_4	1:1	BV_IH1	
				1:2	BV_IH2	
				1:3	BV_IH3	
			CO_2	–	BV_IC	

among a set of choices. This algorithm relies on pairwise comparisons of options, where the option receiving the most support against others is declared the winner. The Condorcet algorithm is designed to analyze decision-making scenarios and optimal strategies. The Condorcet algorithm specifically finds applications in prioritizing choices and making decisions involving multiple options and stakeholders. The Condorcet algorithm is often used to address group selection problems, particularly when conflicting criteria are present. This method can prioritize options based on a comparative evaluation of criteria (Felsenthal and Machover 1998; Tideman et al. 2006; Akhavan et al. 2023). This study employed the Condorcet algorithm within the framework of game theory to prioritize and optimally select 62 applicable MGPC samples derived from various sources. The genetically modified porous carbon samples were comprehensively compared based on 12 key criteria, namely, (1) Point surface area at p/p° ($m^2\ g^{-1}$), (2) BET surface area ($m^2\ g^{-1}$), (3) Langmuir surface area, (4) t-plot external surface area, (5) BJH (Barrett-Joyner-Holland index) adsorption cumulative surface area, (6) BJH desorption cumulative surface area, (7) t-plot micropore volume, (8) BJH desorption cumulative volume, (9) BJH adsorption mean pore width (4V/A), (10) BJH desorption mean pore width (4V/A), (11) Cumulative surface area of pores ($m^2\ g^{-1}$), and (12) Mean pore hydraulic radius (V/A) directly affecting the MGPC performance in soil and water conservation and agricultural productivity (Akhavan et al. 2023). For each criterion, an initial weighting indicated the relative importance of that criterion in achieving the project objectives. In the next step, pairwise comparisons were performed among all 62 samples. In this comparison of how the Condorcet decision-making algorithm was used to select the most optimal sample, a decision matrix was first created based on technical criteria (such as specific surface area, pore volume, structural stability, production efficiency, etc.). If the units of the criteria were different, the min–max normalization method was used to standardize the data. Then, pairwise comparisons were made between all options, such that for each pair of options, the number of criteria for which one option performed better than the other was calculated according to the weight of each criterion. The weighting of the criteria was determined based on expert opinion and pairwise comparisons to assess their relative importance in the decision-making process. In this algorithm, an option is selected as the final winner that performs better than all other options in a pairwise comparison (i.e., the dominant option or Condorcet Winner). In cases where preference cycles between options were established and it was not possible to identify a clear winner (a phenomenon known as Condorcet's paradox), the Borda Count method was used for alternative ranking, whereby options were prioritized based on the sum of the points they obtained from their rankings in pairwise comparisons. This procedure enables a final decision to be made, even in the presence of conflict or uncertainty regarding the relative superiority of the options.

3 Results and discussion

As mentioned above, eight raw materials were used to produce initial biochar. The produced biochars were then subjected to three activators (i.e., KOH and H_3PO_4 in three levels and CO_2 in one level). As shown in Table 2, 64 samples (i.e., eight initial biochar, 24 KOH-activated, 24 H_3PO_4-activated, and 8 CO_2-activated) were ultimately prepared, two of which did not produce appropriate products for further analyses.

3.1 BET analyses

Table 2 presents the BET analysis results for MGPC derived from various materials. It also provides a comprehensive set of physical and surface properties (e.g., surface area, adsorption mean pore diameter, total pore volume, and t-plot micropore volume) of porous carbons

produced from diverse bio-sources (i.e., rice straw, palm pruning waste, vineyard pruning waste, sawdust, poultry slaughterhouse waste, paper mill residues, and tissue paper manufacturing by-products). The BET surface area, adsorption mean pore diameter, total pore volume, and t-plot micropore volume were included in the BET analysis. A detailed analysis of these data demonstrates the impact of bio-sources, production process conditions, and structural modifications on the porous properties of these materials. Overall, BET analysis results show that parameters such as specific surface area, pore volume, and mean pore diameter highlight the influence of structural changes and genetic modifications. In the present study, to produce and select optimal MGPC samples, the use of BET parameters, especially pore volume (t-plot), has been prioritized because these parameters, such as specific surface area and pore volume, have a direct and fundamental relationship with the physical structure of carbon materials and indicate the amount of space available for physical water and nutrient absorption. These characteristics play a fundamental role in improving soil moisture retention capacity and nutrient absorption and are the basis for the initial evaluation of the functional potential of these materials. In addition, the pore volume extracted through t-plot analysis provides valuable information about microscopic pores that play a decisive role in physical absorption and is considered a suitable criterion for prioritizing research samples. Finally, since field performance data are not yet available, focusing on BET parameters enables the identification and selection of samples with optimal structures, a prerequisite for more comprehensive performance evaluations in subsequent stages. Therefore, prioritizing BET parameters at this stage of research is a scientific approach that aligns with the research objectives and provides a solid foundation for the development and completion of applied studies (Kwiatkowski and Broniek 2020). Enhancing these critical factors improves the performance of porous carbons in molecular adsorption, energy storage, and catalytic applications, making them suitable for various purposes, particularly in soil and water conservation. The findings underscore that those materials with higher specific surface area and pore volume, such as B_RSK_2 and B_SDK_1, exhibit superior performance. Additionally, cellulosic bio-sources, such as rice straw and sawdust, showed better performance in producing porous carbons with balanced structures. Scientific analysis of BET results further reveals that the porous properties of produced carbons are highly dependent on the bio-source and production process conditions. Optimizing activation conditions, such as temperature, duration, and chemical activators, can significantly enhance specific surface area and pore volume. The results of this study emphasize the importance of materials with high specific surface area and pore volume for applications in adsorption, catalysis, energy storage, and the conservation of the quantity and quality of soil and water.

The BET surface area is one of the most critical characteristics of porous carbons, representing the material's ability to establish surface interactions with gases, liquids, and dissolved molecules. In this study, the BET surface area ranged from 3.15 $m^2\ g^{-1}$ for BR_S to 1071.47 $m^2\ g^{-1}$ for BR_SK_2. The BR_SK_2 sample (carbon derived from rice husk) exhibited the highest BET surface area, indicating that the carbonization and thermal activation processes in this sample were optimized, leading to an extensive porous structure. Samples with very low surface areas, such as BR_S, indicate non-optimal production processes or pore blockage. Insufficient chemical or thermal activation likely failed to open the pores or remove obstructive materials. Comparisons between samples reveal that biomass wastes, such as sawdust (BS_DK_1) and date palm pruning residues (BP_TK_1), also exhibit high surface areas of 846.75 $m^2\ g^{-1}$ and 887.32 $m^2\ g^{-1}$, respectively. This finding highlights the regular cellulose structure and organic richness of these materials, which contribute to the effective formation of pores during carbonization.

Total pore volume is another characteristic that evaluates the material's ability to adsorb various molecules. The pore volumes of the samples ranged from 0.09 $cm^3\ g^{-1}$ to 0.36 $cm^3\ g^{-1}$. A higher pore volume means greater access to the surface and increased capacity to adsorb larger molecules. For instance, the BP_TK_3 sample, with a pore volume of 0.36 $cm^3\ g^{-1}$, exhibited the highest value, demonstrating an extensive porous structure and higher efficiency in molecular adsorption processes. The reduced pore volume in some samples (e.g., BR_S and BS_W) indicates limiting processes, such as pore blockage or structural breakage of the carbon, which negatively affect the adsorption performance.

The mean pore diameter determines the size distribution of pores and the type of porous material (i.e., micro, meso, or macroporous). In this study, the mean pore diameters ranged from 11.8 to 16.3 Å. Larger diameters suggest that the pores in the material can accommodate larger molecules. The BR_SK_1 sample, with a mean pore diameter of 16.3 Å, demonstrated the best performance, indicating a predominantly mesoporous structure. Smaller pore diameters, such as 11.81 Å in the BS_DK_2 sample, indicate a predominantly microporous structure. These materials are more suitable for adsorbing smaller molecules and energy storage. A decrease in pore diameter below 13.2 Å indicates restricted structures that may reduce the adsorption of larger molecules. Materials with

Table 2 BET analysis results of Morph-Genetic Porous Carbon (MGPC)

Sample	point surface area ($m^2 g^{-1}$)	BET surface area ($m^2 g^{-1}$)	Langmuir surface area ($m^2 g^{-1}$)	t–Plot external surface area ($m^2 g^{-1}$)	BJH adsorption cumulative surface area ($m^2 g^{-1}$)	BJH desorption cumulative surface area ($m^2 g^{-1}$)	BJH desorption (Å)	BJH adsorption (Å)	Mean pore hydraulic radius (Å)	Cumulative surface area($m^2 g^{-1}$)	t–Plot micropore volume ($cm^3 g^{-1}$)	BJH desorption ($cm^3 g^{-1}$)
BR_SK_1	599.81	627.96	897.95	103.8711	107.261	119.2	36.15	35.14	3.25	895.29	0.24	0.1
BR_SK_2	1027.68	1,071.47	1,622.33	472.7966	497.008	479.63	26.07	25.81	4.31	1,314.45	0.29	0.31
BR_SK_3	–	–	–	–	–	–	–	–	–	–	–	–
BR_SH_1	410.09	426.8	604.93	84.54	87.56	72.33	30.2	27.99	3.62	610.38	0.16	0.05
BR_SH_2	531.76	554.75	790.79	168.75	180.38	161.56	23.58	23.34	3.87	743.54	0.18	0.09
BR_SH_3	51.64	52.19	99.89	32.07	36.28	35.21	52.29	41.08	5.48	47.26	0	0.04
BR_SC	365.34	378.2	601.81	121.69	133.72	172.18	40.04	39.89	0.16	463.92	0.12	0.17
BR_S	3.078	3.147	23.04	4.15	7.24	6.54	46.62	54.96	0.00	0.00	0.00	0.00
BP_TK_1	805.98	846.75	1,195.81	139.82	143.31	167.99	35.89	32.19	3.15	1,223.18	0.33	0.15
BP_TK_2	834.1	860.54	1,357.73	494.92	491.25	488.46	26.41	25.72	4.4	981.54	0.17	0.32
BP_TK_3	960.47	979.72	1,650.12	757.03	761.34	658.66	25.64	24.78	5.11	1,026.63	0.11	0.42
BP_TH_1	284.61	422	422	63.53	64.07	55.57	27.45	27.24	3.52	420.47	0.11	0.04
BP_TH_2	637.29	663.88	971.64	238.46	246.49	223.85	27.74	27.42	3.73	823.08	0.19	0.15
BP_TH_3	248.55	255.51	398.35	114.2	121.66	118.37	31.98	29.28	4.15	288.42	0.07	0.09
BP_TC	298.11	318.56	–	–	–	–	–	–	–	–	–	–
BP_T	2.58	3.4	−21.47	5.911	9.67	7.98	51.79	51.95	0.00	0.00	0.00	0.01
BS_DK_1	845.08	887.32	1,250.61	148.67	149.9	161.47	32.4	31.77	3.28	1,261.28	0.35	0.13
BS_DK_2	871.6	892.04	1,438.56	635.78	646.31	570.13	28.21	25.52	4.75	933.63	0.12	0.4
BS_DK_3	644.97	672.03	1,003.77	146.17	162.19	211.81	40.32	39.12	3.09	875.41	0.24	0.21
BS_DH_1	–	–	–	–	–	–	–	–	–	–	–	–
BS_DH_2	570	595.7	827.25	130.96	131.6	114.07	24.56	24.15	3.51	821.82	0.22	0.07
BS_DH_3	695.56	726.37	1,049.23	264.23	275.91	247.1	24.01	23.13	3.88	24.02	0.22	0.15
BS_DC	360.27	372.46	591.15	120.83	131.99	163.87	35.62	37.29	4.17	501.89	0.12	0.14
BS_D	24.62	24.61	42.29	7.2	8.33	5.59	42.95	45.57	4.6	35.19	0.00	0.00
BS_WK_1	19.27	20.08	86.1	27.69	27.68	34.21	60.09	47.66	0.00	0.00	0.00	0.05
BS_WK_2	31.91	32.8	102.49	37.13	46.06	43.16	49.72	53.64	0.00	0.00	0.00	0.05
BS_WK_3	33.98	34.92	95.27	38.36	44.64	41.59	49.42	45.37	0.00	0.00	0.00	0.05
BS_WH_1	4.57	4.75	22.51	6.42	8.53	8.58	48.12	48.65	0.00	0.00	0.00	0.01
BS_WH_2	3.57	5.39	−19.88	8.57	13.81	11.42	50.06	50.59	0.00	0.00	0.00	0.01
BS_WH_3	2.31	2.57	42.38	4.25	6.32	5.14	51.97	50.39	0.00	0.00	0.00	0.00
BS_WC	16.06	16.99	71.67	23.05	29.48	32.29	62.23	51.79	0.00	0.00	0.00	0.05
BS_W	0.47	0.11	0.33	1.88	2.76	2.11	46.45	50.99	0.00	0.00	0.00	0.00
BV_IK_1	30.61	31.21	84.17	30.85	37.78	37.99	52.67	53.15	0.00	0.00	0.00	0.05
BV_IK_2	17.47	18.06	54.11	21.18	25.24	22.82	43.05	46.02	0.00	0.00	0.00	0.02

Table 2 (continued)

Sample	point surface area ($m^2 g^{-1}$)	BET surface area ($m^2 g^{-1}$)	Langmuir surface area ($m^2 g^{-1}$)	t–Plot external surface area ($m^2 g^{-1}$)	BJH adsorption cumulative surface area ($m^2 g^{-1}$)	BJH desorption cumulative surface area ($m^2 g^{-1}$)	BJH desorption (Å)	BJH adsorption (Å)	Mean pore hydraulic radius (Å)	Cumulative surface area($m^2 g^{-1}$)	t–Plot micropore volume ($cm^3 g^{-1}$)	BJH desorption ($cm^3 g^{-1}$)
BV_IK_3	30.25	30.99	82.41	32.25	38.07	39.1	45.64	47.85	0.00	0.00	0.00	0.04
BV_IH_1	13.88	13.99	36.25	11.7	14.62	16.99	46.81	51.09	10.58	7.73	0.00	0.01
BV_IH_2	1.69	1.7	8.44	1.76	3.21	3.05	47.22	54.54	0.00	0.00	0.00	0.00
BV_IH_3	0.81	1.71	−2.16	2.07	4.14	3.36	48.27	53	0.00	0.00	0.00	0.00
BV_IC	5.02	5.27	19.46	6.99	8.54	7.63	51.19	45.86	0.00	0.00	0.00	0.00
BV_I	7.28	7.6	22.24	9.11	10.74	10.55	59.56	45.76	0.00	0.00	0.00	0.01
BP_FK1	271.07	277.26	480.05	181.24	194.38	199.82	37.61	32.47	5.82	295.4	0.04	0.19
BP_FK2	22.44	23	64.09	24.84	29.37	30.02	60.88	44.41	0.00	0.00	0.00	0.04
BP_FK3	24.9	25.97	108.84	34.72	43.83	41.68	41.17	48.41	0.00	0.00	0.00	0.04
BP_FH1	7.64	7.77	24.93	8.22	10.48	11.89	39.99	49.69	9.96	0.37	0.00	0.01
BP_FH2	129.88	132.11	233.91	70.97	78.35	77.34	36.55	37.45	5.32	149.01	0.03	0.07
BP_FH3	798.2	831.92	1,202.74	350.42	360.15	294.32	23.63	22.83	4.015	1,029.92	0.23	0.17
BP_FC	53.56	53.92	111.65	34.74	40.79	47.49	56.85	47.16	5.18	38.81	0	0.07
BP_F	1.92	−4.93	−3.52	6.02	9.97	7.65	46.86	50.72	0.00	0.00	0.00	0.00
BT_PK1	596.05	620.32	937.77	155.99	176.15	218.12	43.74	42.84	3.12	745.14	0.22	0.29
BT_PK2	131.42	133.45	257.12	84.75	96.11	117.27	53.2	44.02	3.98	87.51	0.02	0.15
BT_PK3	5.4	5.61	29.48	7.86	10.77	10.01	42.96	50.44	0.00	0.00	0.00	0.01
BT_PH1	26.16	27.02	73.32	30.31	35.06	31.91	42.82	44.96	0.00	0.00	0.00	0.03
BT_PH2	0.81	0.94	−6.05	1.69	3.54	2.83	46.23	53.82	0.00	0.00	0.00	0.00
BT_PH3	0.81	0.94	−6.05	1.69	3.54	2.83	46.23	53.82	0.00	0.00	0.00	0.00
BT_PC	78.64	79.53	143.77	39.11	44.85	54.97	46.69	42.22	3.13	73.35	0.02	0.06
BT_P	6.01	6.37	20.17	8.18	9.82	9.06	64	48.46	0.00	0.00	0.00	0.01
BV_PK1	560.16	560.25	892.86	172.56	191.9	203.93	33.19	34.1	3.82	694.78	0.19	0.17
BV_PK2	641.19	667.49	1,007.94	268.31	284.18	262.05	30.05	27.06	4.12	841.15	0.19	0.19
BV_PK3	4.42	6.18	−37.92	10.19	15.86	12.91	48.56	51.28	0.00	0.00	0.00	0.01
BV_PH1	34.34	34.41	64.32	14.97	17.75	18.73	38.84	44.49	3.47	33.44	0.01	0.02
BV_PH2	188.39	192.87	321.5	77.64	86.87	87.51	35.22	37.92	4.19	216.94	0.05	0.08
BV_PH3	1.09	1.62	−5.16	2.61	4.81	3.78	45.63	52.98	0.00	0.00	0.00	0.00
BV_PC	36.28	36.46	78.99	23.21	27.78	31.26	36.83	43.53	7.33	44.51	0.00	0.03
BV_P	5.51	6.2	184.74	10.58	15.92	12.98	44.87	51.83	0.00	0.00	0.00	0.01

diverse pore size distributions can combine capabilities for adsorbing small and large molecules, making them more effective for multipurpose applications.

This property indicates the presence of pores smaller than 2 nm, which are crucial for adsorbing gases and storing energy. The micropore volumes ranged from 0.009 $cm^3\ g^{-1}$ to 0.35 $cm^3\ g^{-1}$. With high micropore volumes, samples such as BR_SK_2 and BS_DK_1 demonstrated efficiency in adsorbing minor gases, including CO_2 and CH_4. A reduction in this property in samples like BR_S and BS_W suggests that these materials lack sufficient microporous structures and may not be suitable for specific applications.

Studies by Fard et al. (2021), Patel and Panwar (2023), and Zhou et al. (2025) on porous carbons derived from biomass residues emphasized the production of porous carbons from agricultural residues such as rice straw and wood waste. They examined the effects of biomass resources on their BET surface area and pore volume. Their studies revealed that Iranian biomass has a high potential for producing porous carbons with suitable structures. Some studies have shown that the source of raw materials has a significant influence on the structural and physical properties of porous carbons. Zhao et al. (2023) investigated the impact of biomass resources, including rice straw, wood, and industrial waste, on the characteristics of porous carbons. Their findings revealed that carbons produced from cellulosic residues exhibited high BET surface area and pore volume, which could adsorb both small and large molecules also investigated the impact of various raw materials on the properties of porous carbon. They concluded that agricultural residues and biomass increased pore structures due to their higher organic content, which plays a role in activation processes. Chemical and thermal activation processes are essential for improving the pore structure of porous carbons. Sharma et al. (2020) studied activating agents, such as KOH and $ZnCl_2$, which can remove obstructive materials and create new pore structures, thereby enhancing the BET surface area and pore volume. Okoli et al. (2016) examined the effects of chemical activation on the properties of carbons derived from wood waste and reported significant improvements in surface area and pore volume. Porous carbons, with their high surface area and pore volume, are highly effective in energy storage (supercapacitors and batteries), water and air purification, and adsorption of pollutant gases, mainly CO_2. Wang et al. (2019) examined the effects of porous carbons on gas adsorption (e.g., CO_2 and CH_4) and demonstrated that optimized porous structures enhance adsorption performance for small and large molecules. These applications go beyond gas absorption and are also very effective in improving soil quality. Several studies have emphasized that adding activated carbon to soil increases porosity and improves soil structure, thereby enhancing water permeability and promoting better soil ventilation, which helps stabilize soil particles and reduce erosion (Al-Soudany et al. 2018). This helps increase soil-activated carbon and stabilize it in the long term, improving agricultural performance (Chamberlin et al. 2021).

3.2 Priority MGPCs

In the present study, a game theory approach using the Condorcet method has been applied to determine the prioritization and evaluate the efficiency of morph-genetic porous carbon. This method allows the analysis of qualitative and quantitative differences between samples in competitive scenarios. The Condorcet model involves pairwise comparisons, where the option that has achieved the most victories over other options is identified as the winner. The primary feature of this model is the identification of the winner that has the advantage in all or the majority of comparisons. In the case of cycles, the option with the fewest failures is recognized as the final winner. Therefore, using the game theory-based concordance algorithm, the prioritization of 62 genetically modified porous carbon samples was examined based on 12 key criteria related to the project missions (i.e., optimizing MGPC to regulate efficient use of soil and water resources in sloping farmland on the Loess Plateau) and directly impacted the performance and prioritization of the samples. The case-wise ranking of the study samples based on the desired criteria has been summarized in Table 3. Accordingly, the samples under study were initially ranked in each criterion. In this regard, the first rank was assigned to the superior sample, and the last rank was assigned to the last sample from the viewpoint of the study criterion and in interaction with the expected performance for the study purpose. After ranking the samples in each criterion, pairwise comparisons were made between all samples based on their rankings across all criteria. Accordingly, a 62×62 matrix was set up. In this matrix, the samples entered the game in pairs. Each sample that achieved the highest number of wins according to the study criteria was identified as the superior sample and received a point in the matrix. Finally, the score of each sample was determined based on the total number of achieved in the game. The results of the pairwise comparisons and the final comprehensive rankings are reported in Tables 4 and 5.

Analyzing the results of the game theory application helps understand the performance of the samples and identify the superior samples. KOH samples produced by the chemical process showed the highest rank and the best performance. Conventional biochars were ranked

low; the first conventional biochar, ranked 48th, is at a significant distance from the superior samples. Furthermore, biochars activated by chemical processes using KOH and H_3PO_4 and those exposed to CO_2 gas ranked high. These results indicate that conventional biochars cannot meet the project's expected requirements in terms of both qualitative and quantitative criteria. The difference in scores showed that the superior KOH samples not only had a higher number of wins but also had a significant difference in most cases.

The findings of this study are consistent with the results of previous studies. For instance, Tang et al. (2021) have emphasized that the chemical activation process using KOH and H_3PO_4 significantly enhances the quality of biochar, particularly in terms of adsorption capacity and structural stability. Lehmann et al. (2006) have also shown that conventional biochars have a lower ability in specific applications, such as soil improvement and carbon sequestration, due to their less developed structural characteristics. These findings indicate that the samples produced by chemical activation methods have shown much better performance than conventional samples. After applying game theory and analyzing the available strategies, five priority samples, including BP_TK_2, BR_SK_2, BS_DK_2, BT_PK_2, and BV_PK_2, were selected from the studied options, whose BET results are illustrated in Fig. 4.

The graphs in Fig. 3 illustrate the adsorption and desorption behavior of a porous material as a function of relative pressure and the amount adsorbed. Additionally, the determination of the pore size (Fig. 4) provides more detailed information about the material's structural characteristics. A closer analysis reveals that in BP_TK_2, the main graph illustrates the relationship between the amount of adsorbed gas ($cm^3\ g^{-1}$STP) and the relative pressure (0p/p). This figure resembles a type IV isotherm, which is related to the mesoporous structure of the material. At low relative pressures (< 0.4), the adsorption amount increases continuously, which is related to the initial molecular adsorption on the inner walls of the pores. This stage involves gas adsorption as monolayers or multilayers on the surface. In contrast, at higher relative pressures (> 0.4), a sharp increase in adsorption is observed, indicating an increase in pressure within the mesoporous structure of the material. The hysteresis loop is visible in the relative pressure region between 0.4 and 1.0. This loop is typically associated with a slower desorption rate than adsorption due to capillary action within the drilled pores. This behavior is typical for materials with uniformly sized mesoporous structures. The small graph in the image illustrates the pore size distribution, which is based on the variation of pore volume with pore width (dV/dw). This graph indicates that the pores in the material are predominantly in the range of 12 to 18 Å, with a relatively uniform pore size distribution throughout the material and a peak in the same range. As the pore width increases beyond 18 Å, the dV/dw value decreases, indicating a decrease in the contribution from pores larger than 18 Å. This behavior suggests that the material comprises uniformly sized mesopores with fewer micropores or macropores. A Type IV isotherm and hysteresis loop indicate a structure with mesoporous pores suitable for various applications. The uniformity of pore size generation, ranging from 12 to 18 Å, demonstrates that the material can be optimized for processes such as gas adsorption, energy storage, or molecular separation (Fig. 4).

In BR_SK_2, the adsorption curve increases steeply in the low relative pressure regions. This stage indicates the presence of tiny pores and the openness of gas adsorption pathways. At approximately 0.4, the slope of the curve decreases and continues to decrease with increasing pressure relative to the saturation pressure. This indicates the beginning of saturation of the material, meaning that most of the tiny pores are filled, and the adsorption capacity approaches its maximum. As the pressure increases, the desorption curve gradually decreases in slope. This trend indicates the material's resistance to gas desorption from its pores. The desorption curve has a lower slope than the adsorption curve, indicating the presence of gas traps in the pores. Gases that have been adsorbed gradually leave the material as the pressure increases below the initial value. The gap between the adsorption and desorption curves indicates that the adsorption and desorption capacities do not overlap and that the adsorption and desorption processes follow different mechanisms, resulting in hysteresis. The small graph in the image indicates that the highest adsorption rate occurs at pore widths of approximately 6 to 12 Å. This indicates that pores of this size have the highest adsorption capacity. As the pore width increases, the adsorption rate decreases sharply. This decrease indicates that gases cannot quickly enter pores of larger sizes. As a result, the adsorption efficiency in these pores decreases (Fig. 4). In BS_DK_2, the graph shows that the adsorption increases nonlinearly with increasing partial pressure and reaches saturation near a partial pressure of 1. This behavior is usually observed in materials with a porous structure and a limited adsorption capacity. The amount of substance released during the pressure reduction process is shown. The release curve is typically lower than the adsorption curve, indicating hysteresis (a delay) between the adsorption and release processes. This phenomenon depends on the material's structural characteristics and the intermolecular forces it exhibits. The peak at about 6 Å indicates that pores of this size provide the highest adsorption capacity. As the pore size increases, the adsorption capacity decreases, indicating a decrease

Table 3 Ranking of study samples in each of the desired criteria

Sample	Criterion											
	1	**2**	**3**	**4**	**5**	**6**	**7**	**8**	**9**	**10**	**11**	**12**
1	2	2	62	18	18	18	13	18	7	54	2	8
2	18	18	18	25	25	25	10	25	59	37	24	12
3	25	25	2	17	2	17	11	17	51	40	16	14
4	24	24	25	2	17	2	14	2	33	32	44	11
5	17	17	17	44	44	44	12	47	55	62	18	58
6	16	16	24	9	9	9	8	26	60	45	17	42
7	44	44	44	29	29	29	24	9	49	48	25	39
8	29	29	16	20	20	20	16	39	23	55	1	5
9	27	27	29	27	27	47	2	44	15	5	26	43
10	26	26	9	8	39	26	26	6	37	23	9	45
11	9	9	26	39	8	39	1	8	58	61	20	18
12	20	20	20	4	4	8	44	48	38	36	28	25
13	1	1	27	47	47	6	29	20	46	33	47	31
14	47	47	47	24	26	27	27	16	36	34	4	17
15	28	28	1	26	24	16	28	29	52	60	3	2
16	8	8	8	16	16	30	47	30	42	35	30	30
17	4	4	28	28	6	4	20	24	35	59	6	21
18	3	3	4	6	30	24	9	1	54	46	19	9
19	6	19	3	30	28	1	4	27	41	58	22	44
20	30	6	6	21	21	21	17	4	57	53	39	48
21	19	30	30	1	1	48	3	21	32	7	21	29
22	39	39	39	12	48	28	25	12	45	38	43	4
23	21	21	19	48	3	12	6	43	56	51	48	27
24	22	22	21	3	12	43	30	28	61	49	53	20
25	12	12	22	43	43	3	19	45	62	57	5	3
26	48	48	12	19	19	19	18	53	31	15	45	19
27	43	43	48	22	22	53	22	3	34	47	31	28
28	53	53	43	53	49	45	21	33	50	56	29	22
29	45	45	15	34	33	22	39	34	40	52	27	24
30	5	5	53	53	53	33	43	32	48	31	58	1
31	14	14	49	49	34	49	48	37	47	50	14	16
32	11	34	45	45	41	41	53	55	53	41	12	53
33	34	11	41	41	45	34	5	49	5	26	8	47
34	33	33	33	57	57	57	45	5	6	6	11	26
35	55	55	5	5	55	55	31	40	26	42	42	6
36	57	57	34	14	5	5	58	57	43	39	7	7
37	50	20	32	55	50	32	55	41	30	43	10	10
38	41	41	55	50	37	37	59	19	1	1	13	13
39	31	31	57	32	40	50	42	22	22	16	15	15
40	40	49	14	40	14	40	51	50	39	30	23	23
41	49	40	50	37	32	14	7	14	16	22	32	32
42	32	32	37	56	56	56	60	56	24	24	33	33
43	56	56	11	11	11	58	38	58	21	21	34	34
44	37	37	40	10	15	11	57	11	3	3	35	35
45	58	58	56	58	10	15	62	62	20	9	36	36
46	42	42	31	15	58	42	35	10	19	25	37	37
47	62	62	58	62	36	36	61	15	9	20	38	38
48	54	54	52	36	52	62	54	54	2	19	40	40

Table 3 (continued)

Sample	Criterion											
	1	2	3	4	5	6	7	8	9	10	11	12
49	15	15	42	42	62	10	40	36	17	17	41	41
50	52	10	7	54	42	52	52	42	25	2	46	46
51	61	52	35	52	46	54	23	52	18	18	49	49
52	35	36	54	31	54	35	56	23	28	28	50	50
53	10	61	61	61	23	23	50	35	4	29	51	51
54	36	35	59	35	61	46	34	61	29	44	52	52
55	7	23	38	46	35	61	46	46	44	4	54	54
56	23	7	60	23	31	7	33	7	8	27	55	55
57	46	60	46	7	7	31	36	31	27	12	56	56
58	59	59	13	13	13	60	15	13	12	8	57	57
59	13	13	51	60	60	59	37	60	11	10	59	59
60	60	51	36	38	51	51	32	59	14	11	60	60
61	51	38	23	59	59	13	41	51	13	13	61	61
62	38	46	10	51	38	38	49	38	10	14	62	62

Features used to prioritize Morph-Genetic Porous Carbon samples (1) Point surface area at p/p° (m^2/g), (2) BET surface area (m^2/g), (3) Langmuir surface area, (4) t-Plot external surface area, (5) BJH adsorption cumulative surface area, (6) BJH desorption cumulative surface area, (7) t-Plot micropore volume, (8) BJH desorption cumulative volume, (9) BJH adsorption mean pore width (4 V/A), (10) 9BJH desorption mean pore width (4 V/A), (11) Cumulative surface area of pores (m^2/g), (12) Mean pore hydraulic radius (V/A)

in the efficiency of larger pores in the adsorption process. The material under study has a significant capacity for adsorption at high pressures, and the adsorption process reaches saturation. The hysteresis between adsorption and release indicates the porous structure and specific surface properties of the material (Fig. 4).

In BV_PK_2, the adsorption curve, represented by black squares, shows a nonlinear increase in the amount of gas adsorbed with increasing relative pressure. Adsorption starts significantly at low pressures and reaches saturation near 1, a behavior attributed to the gradual filling of the material's pores. The release curve, marked by red circles, shows the gas released from the material during the pressure reduction process. The curve is located below the adsorption, indicating hysteresis. This phenomenon is typically observed in materials with mesopores (2–50 nm) or micropores and is related to strong intermolecular forces or a complex material structure. A clear peak is observed at the pore width of about 6 Å, indicating the crucial role of this size in the adsorption process, as these pores provide the highest gas adsorption. Beyond 6 Å, the adsorption rate decreases sharply (Fig. 4).

The graph associated with BT_PK2 shows the gas adsorption and desorption isotherm for a porous material, which presents the volume of adsorbed gas as a function of the relative pressure. The adsorption and desorption curves are marked with square and circular dots. The hysteresis loop observed in this isotherm usually indicates the presence of mesoporous pores (pores with a size of 2–50 nm) and is considered a type IV isotherm. The smaller graph in the figure displays the pore size distribution, which illustrates the pore volume as a function of pore width. At low relative pressures, the gradual increase in the adsorbed volume is due to the formation of a monomolecular layer on the surface of the material. At moderate relative pressures, multilayer adsorption occurs in the pores. A sharp increase in adsorption is observed at high relative pressures due to vapor condensation in the pores. The hysteresis loop between the adsorption and desorption paths reflects the specific features of the mesoporous structure and gas evaporation in the pores. The smaller plot indicates that most pores have a width of approximately 10–12 Å, confirming that the material exhibits a dominant mesoporous structure. The volume of larger pores (> 20 Å) is lower, indicating a concentration of pores in the mesoporous range (Fig. 4).

Sing (1984) demonstrated that this decrease in the slope of the desorption curve is attributed to the presence of gas in the larger pores, which prevent the rapid escape of gases. Similar results were also reported by Rouquerol et al. (1999), who showed that hysteresis loops are common in materials with uniform mesoporous structures and are dependent on the capillary behavior of the pores. The small graph in the image shows that the highest adsorption rate is observed in the pore size range of 6 to 12 Å. In general, Wang et al. (2018) demonstrated that at higher pressures, the faster filling of larger pores and the formation of liquid within the pores prevail. This

Table 4 Comparison matrix between study samples and game theory score

	1	2	3	4	5	6	7	8	9	10	11	12	13	14	15	16	17	18	19	20	21	22	23	24	25	26	27	28	29	30	31	32
1	*	2	1			*	1	*	9	1						16	17	18	1	20	1			24	25	26	27	1	29	*	1	
2	2	*	2							2						2	2	*	2	2	2	2	2	2	*	2						
3	1	2	*	4	3	*	3	8	9	3						16	17	18	3	20	21	3	3	24	25	26	27	28	29	30	3	
4	1	2	4	*	4			8	9	4						16	17	18	4	20	4	4	4	24	25	26	27	28	29	4	4	4
5	1	2	3	4	*	6	5	8	9	5		12		5		16	17	18	19	20	21	22	5	24	25	26	27	28	29	30	5	
6	*	2	*	4	6	*	6	8	9	6						16	17	18	6	20	6	22	23	6	25	26	*	*	29	6		
7	1	2	3	4	5	6	*	8	9	10	11	12	7	14	*	16	17	18	19	20	21	22	23	24	25	26	27	28	29	30	31	7
8	*	2	8					*	9	8						17	18	8	20	8	8	8	8	25	26	*	*	29	8			
9	9	2	9						*	9	9	9	9	9	*	17	18	9	9	9	9	9	*	25	26	9						
10	1	2	3	4	5	6	10	8	9	*	11	12	10	14	15	16	17	18	19	20	21	22	10	24	25	26	27	28	29	30	*	32
11	1	2	3	4	5	6	11	8	9	11	*	12	11	14	11	16	17	18	19	20	21	22	11	24	25	26	27	28	29	30	11	32
12	1	2	3	4	12	6	12	8	9	12		*		12		16	17	18	12	20	21	12	12	24	25	26	27	28	29	30	12	
13	1	2	3	4	5	6	7	8	9	10	11	12	*	14	15	16	17	18	19	20	21	22	23	24	25	26	27	28	29	30	31	32
14	1	2	3	4	5	6	14	8	9	14		12	14	*	14	16	17	18	19	20	21	22	14	24	25	26	27	28	29	30	14	
15	1	2	3	4	5	6	*	8	9	15	11	12	15	14	*	16	17	18	19	20	21	22	15	24	25	26	27	28	29	30	*	32
16	16	2	16					8	*	16						*	17	18	16	*	16			24	25	26	16					
17	17	2	17													*	18	17						24	25	17						
18	18	*	18													*	18	*	20	21	19			24	25	26	27	28	29	30	19	
19	1	2	3	4	19	6	19	8	9	19		12		19		16	17	18	20	*	20			*	25	26	27	28	29	30	19	
20	20	2	20						9	20						*	17	18	20	*	20			*	25	26			29	20		
21	1	2	21	4	21	6	21	8	9	21						16	17	18	21	20	*	21		24	25	26	27	*	29	30	21	
22	1	2	3	4	22			8	9	22		12		22		16	17	18	19	20	21	*	22	24	25	26	27	28	29	30	22	
23	1	2	3	4	5	23		8	9	10	11	12	23	14	15	16	17	18	19	20	21	22	*	24	25	26	27	28	29	30	*	32
24	24	2	24			6	24	8	*	24								18	24	*	24			*	25	*	24		*	*	24	
25	25	*	25															18	25					*	25				25			
26	26	2	26													17	18	26					*	25	*	*	26	*	26			
27	27	2	27			*	27	*	9	27						16	17	18	27	26	27			24	25	*	*	27	29	*	27	
28	1	2	28			*	28	*	9	28						16	17	18	28	26	*	28		24	25	26	27	*	29	30	28	
29	29	2	29						9	29						16	17	18	29	29	29			*	25	*	29		*	29		
30	*	2	30	4	30	6	30	8	9	30						16	17	18	30	20	30			*	25	26	*	30	29	*	30	
31	1	2	3	4	5	6	31	8	9	*	11	12	31	14	*	16	17	18	19	20	21	22	*	24	25	26	27	28	29	30	*	*
32	1	2	3	4	5	6	7	8	9	32	32	12	32	14	32	16	17	18	19	20	21	22	32	24	25	26	27	28	29	30	*	*
33	1	2	3	4	*	6	33	8	9	33	*	12	33	*	33	16	17	18	19	20	21	22	33	24	25	26	27	28	29	30	33	
34	1	2	3	4	5	6	34	8	9	34	34	12	34	*	34	16	17	18	19	20	21	22	*	24	25	26	27	28	29	30	34	35
35	1	2	3	4	5	6	35	8	9	10	11	12	35	14	15	16	17	18	19	20	21	22	23	24	25	26	27	28	29	30	35	32
36	1	2	3	4	5	6	36	8	9	10	11	12	36	14	15	16	17	18	19	20	21	22	*	24	25	26	27	28	29	30	*	32
37	1	2	3	4	5	6	37	8	9	37	*	12	37	*	37	16	17	18	19	20	21	22	37	24	25	26	27	28	29	30	*	32
38	1	2	3	4	5	6	7	8	9	10	11	12	13	14	15	16	17	18	19	20	21	22	23	24	25	26	27	28	29	30	31	32
39	*	2	39			*	39	8	9	39						16	17	18	20	39	39	39	39	25	26	39		*	39			
40	1	2	3	4	5	6	40	8	9	40		12	40	*	40	16	17	18	20	21	22	40	24	25	26	40	27	28	29	30	31	40
41	1	2	3	4	5	6	41	8	9	41	*	12	41	*	41	16	17	18	20	21	22	41	24	25	26	27	28	29	30		41	
42	1	2	3	4	5	6	42	8	9	42	11	12	42	14	*	16	17	18	20	21	22	42	24	25	26	26	27	28	29	30	42	32
43	1	2	3	4	43	6	43	8	9	43		12		43		16	17	18	20	21	43		24	25	26	26	27	28	29	30	43	
44	44	2	44													16	17	18	44				*	25	44							
45	1	2	3	4	45	6	45	8	9	45		12		45		16	17	18	19	20	21	*	45	24	25	26	27	28	29	30	45	
46	1	2	3	4	46	6	46	8	9	10	11	12	46	14	15	16	17	18	19	20	21	22	23	24	25	26	27	28	29	30	*	32
47	47	2	47						9	47							17	18	47	20	21	47	47	47	25	47	*	47	29	47		
48	1	2	48	4	48	6	48	8	9	48						16	17	18	48	20	21	48		24	25	26	*	*	*	30	48	
49	1	2	3	4	*	6	49	8	9	49	*	12	49	*	49	16	17	18	19	20	21	22	49	24	25	26	27	28	29	30	*	49
50	1	2	3	4	5	6	7	8	9	50	*	12	50	*	50	16	17	18	19	20	21	22	50	24	25	26	27	28	29	30	*	50
51	1	2	3	4	5	6	7	8	9	10	11	12	13	14	15	16	17	18	19	20	21	22	23	24	25	26	27	28	29	30	31	32
52	1	2	3	4	5	6	*	8	9	10	11	12	52	14	15	16	17	18	19	20	21	22	52	24	25	26	27	28	29	30	52	32
53	1	2	3	4	53	6	53	8	9	53		12		53		16	17	18	19	20	21	22	53	24	25	26	27	28	29	30	53	
54	1	2	3	4	5	6	55	8	9	10	11	12		54		16	17	18	19	20	21	22	54	24	25	26	27	28	29	30	54	32
55	1	2	3	4	5	6	56	8	9	55	*	12	55	55	55	16	17	18	19	20	21	22	55	24	25	26	27	28	29	30	55	
56	1	2	3	4	5	6	*	8	9	56		12	56	14	56	16	17	18	19	20	21	22	*	24	25	26	27	28	29	30	*	32
57	1	2	3	4	5	6	*	8	9	57	*	12	57	*	57	16	17	18	19	20	21	22	57	24	25	26	27	28	29	30	57	57
58	1	2	3	4	5	6	58	8	9	58	*	12	58	14	58	16	17	18	19	20	21	22	58	24	25	26	27	28	29	30	58	32
59	1	2	3	4	5	6	7	8	9	10	11	12	59	14	15	16	17	18	19	20	21	22	23	24	25	26	27	28	29	30	31	32
60	1	2	3	4	5	6	7	8	9	10	11	12	13	14	15	16	17	18	19	20	21	22	23	24	25	26	27	28	29	30	31	32
61	1	2	3	4	5	6	61	8	9	10	11	12	61	14	15	16	17	18	19	20	21	22	23	24	25	26	27	28	29	30	*	32
62	1	2	3	4	5	6	62	8	9	62	11	12	62	14	62	16	17	18	19	20	21	22	62	24	25	26	27	28	29	30	31	32
Win-Count	44	59	39	44	30	41	7	48	53	14	18	38	2	20	16	51	58	60	36	51	42	34	9	48	59	37	44	41	50	43	8	21
Equal	4	2	1	0	2	4	4	3	2	3	8	0	0	8	1	2	0	1	0	2	1	1	4	6	1	3	6	4	4	3	11	3
Total	92	120	79	88	62	86	18	99	108	31	44	76	4	48	33	104	116	121	72	104	85	69	22	102	119	77	94	86	104	89	27	45

is also observed in the present study, indicating that our material exhibits similar behavior. Zhu et al. (2018) confirmed that this pore size range increases the efficiency of gas adsorption. As the pore size increases, the adsorption rate decreases sharply. The gradual decrease in the desorption curve after saturation indicates the material's resistance to gas escape from the pores. This finding is consistent with Zhao et al. (2020), who also demonstrated that this pore size range exhibits the highest adsorption capacity. They further explained that the lower slope in the desorption curve is due to resistance to gas escape from the larger pores.

It is worth mentioning that the selection of the KOH activator over other activators was associated with comprehensive study properties, particularly the specific surface area obtained using the BET assessment. In this process, various criteria related to the performance of the activators were quantitatively weighted, and the

Table 4 (continued)

	34	35	36	37	38	39	40	41	42	43	44	45	46	47	48	49	50	51	52	53	54	55	56	57	58	59	60	61	62
1	1					*	1				44	1		47	1														
2	2																												
3	3					39	3				44	3		47	48	3													
4	4					39	4				44	4		47	4														
5	5					39	5			43	44	45	46	47	48	*	5			53	5								
6	6					*	6				44	6		47	6														
7	34	35	36	37	7	39	40	41	42	43	44	45	46	47	48	49	7	6	*	53	55	56	*	*	58	6		61	62
8	8										44	8		47	8														
9	9										44	9																	
10	34	10		37	10	39	40	41	42	43	44	45	10	47	48	49	50	10		53	10	55	56	57	58	10			62
11	34	11		*	11	39	40	*	11	43	44	45	11	47	48	*	*	11		53	11	*	56	*	*	11			
12	12					39	12				44	12	12	47	48	12													
13	34	35	36	37	13	39	40	41	42	43	44	45	46	47	48	49	50	13	52	53	54	55	56	57	58	59	13	61	62
14	*	14	14	*	14	39	*	*	14	43	44	45	14	47	48	*	*	14		53	54	55	14	*	14				
15	34	15	15	37	15	39	40	41	*	43	44	45	15	47	48	49	50	15		53	54	55	56	57	58	15			62
16	16													47	16														
17	17																												
18	18																												
19	19					39	19			43	44	19		47	48	19													
20	20										44	20																	
21	21					39	21				44	21																	
22	22					39	22			43	44	*	22	47	48	22													
23	*	23	36	37	23	39	40	41	42	43	44	45	23	47	48	49	50	23	52	53	54	55	*	57	58	23			62
24	24					39	24				*	24		47	24														
25	25																												
26	26										44	26		47	26														
27	27										44	27		*	*	27													
28	28					39	28				44	28		47	*	28													
29	29					*	29				44	29		29	*	29													
30	30					39	30				44	30		47	30														
31	34	35	*	*	31	39	31	41	42	43	44	45	*	47	48	*	*	31	52	53	54	55	*	57	58	31		*	31
32	35	32				39	40	41	32	43	44	45	32	47	48	49	50	32		53	32	55	32	57	32				
33	33					39	33			43	44	45	33	47	48	33				53	33								
34	34					39	34				44	45	34	47	48	34				53	34								
35	34	*	36	37	35	39	40	41	42	43	44	45	35	47	48	49	50	35	*	53	54	55	56	57	58	35	35	61	62
36	34	36	*	37	36	39	40	41	*	43	44	45	36	47	48	49	50	36	36	53	36	55	56	57	58	36	60	61	62
37	34	37		*	37	39	37	37		43	44	45	37	47	48	49	37			53	37	55	37	57	37				
38	34	35	36	37	*	39	40	41	42	43	44	45	46	47	48	49	50	51	52	53	54	55	56	57	58	59	60	61	62
39	39					39					44	39	39	47	39														
40	34	40	40	37	40	39	*	41	42	43	44	45	40	47	48	49	50	40		53	40	55	40	57	40				
41	34	41		37	41	39	41	*	41	43	44	45	41	47	48	49	40			53	54	55	40	57	*	40			
42	34	42	*	37	42	39	42	41	*	43	44	45	42	47	48	49	50	41	41	53	41	55	56	57	58	41			
43	34	43				39	43			*	44	43	43	47	48	43													
44	44										*	44																	
45	45					39	45			43	44	*	45	47	48	45				53	45								
46	34	35	36	37	46	39	40	41	42	43	44	45	*	47	48	49	50	46	52	53	54	55	*	*	58	46		*	62
47	47													*	47														
48	48					39	48				44	48		47	*	48													
49	34	49				39	49			43	44	45	49	47	48	*	49			53	49								
50	34	50		37	50	39	50	40	50	43	44	45	50	47	48	49	*	50		53	50	55	50	57	*	50			
51	34	35	36	37	51	39	40		41	43	44	45	46	47	48	49	50	*	*	53	*	55	*	*	58	59	60	61	62
52	34	52	36	37	52	39			41	43	44	45	*	47	48	49	50	*	*	53						52	60	61	52
53	53					39	53			43	44	53		47	48	53			*	53									
54	34	54	36	37	54	39	40	54	41	43	44	45	54	47	48	49	50	*		*	55	*	54	58	54				62
55	34	55				39	55			43	44	45	55	47	48	49	55			55	*	55							
56	34	56		37	56	39	40		56	43	44	45	*	47	48	49	50	*	53	54	55	*	56	*	56				
57	34	57				39	57			43	44	45	*	47	48	49	57	*		54	55	56	*	*	57				
58	34	58		37	58	39	40	*	58	43	44	45	58	47	48	49	*	58		58	55	*	*	*	58				
59	34	35	36	37	59	39			41	43	44	45	46	47	48	49	50	59	52	53	54	55	56	57	58	*	60	59	
60	34	35	60	37	60	39	40		41	43	44	45	46	47	48	49	50	60		53	54	55	56	57	58	60	*	61	60
61	34	61		37	61	39			41	43	44	45	*	47	48	49	50	61	61	53	54	55	56	57	58	60	61		62
62	34	62		37	62	39			41	43	44	45	62	47	48	49	50	52		53	62	55	56	57	58	60	62		*
Win-Count	28	37	9	20	0	47	20	12	8	37	55	33	5	52	41	25	18	1	6	33	13	24	13	14	16	2	4	8	12
Equal	2			3	0	3	2	7	2		1		5	1	3	6	9	4	3	0	1		8	8	5	0	2		
Total	58	76	20	43	0	97	42	31	18	75	111	67	15	105	85	56	45	6	15	66	27	49	34	36	37	4	10	18	26

optimal activator was prioritized and selected using the Condorcet algorithm. This multi-criteria approach enabled accurate decision-making based on multidimensional data. In addition, the results showed that almost all samples activated with different KOH levels were grouped among the optimal samples, with insignificant differences. Therefore, to optimize material consumption, reduce costs, and facilitate the process, KOH level

Table 5 Prioritizing study samples based on a game theory approach

Sample	Rank	Winner	Equal	Score
BP_TK_3	1	60	1	121
BR_SK_2	2	59	2	120
BS_DK_2	3	59	1	119
BP_TK_2	4	58	0	116
BP_FH_3	5	55	1	111
BV_PK_2	6	53	2	108
BT_PK_1	7	52	1	105
BP_TK_1	8	51	2	104
BP_TH_2	9	51	2	104
BS_DH_3	10	50	4	104
BS_DK_1	11	48	6	102
BV_PK_1	12	48	3	99
BP_FK_1	13	47	3	97
BS_DH_1	14	44	6	94
BR_SK_1	15	44	4	92
BS_DC	16	43	3	89
BR_SH_2	17	44	0	88
BR_SC	18	41	4	86
BS_DH_2	19	41	4	86
BP_TH_3	20	42	1	85
BT_PK_2	21	41	3	85
BR_SH_1	22	39	1	79
BS_DK_3	23	37	3	77
BV_PH_2	24	38	0	76
BS_WH_1	25	37	2	76
BP_FH_2	26	37	1	75
BP_TH_1	27	36	0	72
BP_TC	28	34	1	69
BP_FC	29	33	1	67
BT_PC	30	33	0	66
BR_SH_3	31	30	2	62
BS_WK_2	32	29	2	60
BS_WK_3	33	28	2	58
BT_PK_3	34	25	6	56
BV_IK_1	35	24	1	49
BV_PC	36	20	8	48
BS_WK_1	37	21	3	45
BT_PH_1	38	18	9	45
BV_PH_1	39	18	8	44
BS_WC	40	20	3	43
BP_FK_2	41	20	2	42
BV_IH_1	42	16	5	37
BV_IK_3	43	14	8	36
BV_IK_2	44	13	8	34
BVP	45	16	1	33
BV_PK_3	46	14	3	31
BP_FK_3	47	12	7	31
BSD	48	8	11	27
BTP	49	13	1	27
BVI	50	12	2	26
BPT	51	9	4	22
BS_WH_2	52	9	2	20
BRS	53	7	4	18
BP_FH_1	54	8	2	18
BV_IC	55	8	2	18
BPF	56	5	5	15
BT_PH_3	57	6	3	15
BV_IH_3	58	4	2	10
BT_PH_2	59	1	4	6
BV_PH_3	60	2	0	4
BV_IH_2	61	2	0	4
BSW	62	0	0	0

1 is recommended for activating the produced biochar. The combination of experimental data, specific property analysis, and weighting within the framework of the Condorcet algorithm provided a scientific and coherent basis for selecting the KOH activator and determining its optimal level.

4 Conclusion

The present study provides a detailed analysis of the performance of 62 MGPC samples using the Condorcet game theory method with a weighting of the difference in scores. In this method, game theory, as a powerful MCDM tool, has enabled a detailed and comprehensive evaluation of various options and has ultimately led to the selection of prioritized samples with the highest performance. This systematic approach, which integrates comprehensive physical and chemical data from parameters extracted from BET analysis, provides a scientific and reliable framework for evaluating and prioritizing porous materials. This framework can help optimize the production and application of biochar in various fields, particularly in protecting soil and water resources. The results of this study demonstrate the importance of carefully selecting raw materials and optimizing biochar production processes. The appropriate selection of raw materials for biochar production has a significant impact on the physical, chemical, and functional properties of the final product. In addition, the comparison of the performance of MGPC and conventional biochar has shown the high potential of MGPC for study. Therefore, this approach can be an effective tool in future research in the design and optimization of advanced materials, especially in the agricultural, industrial, and

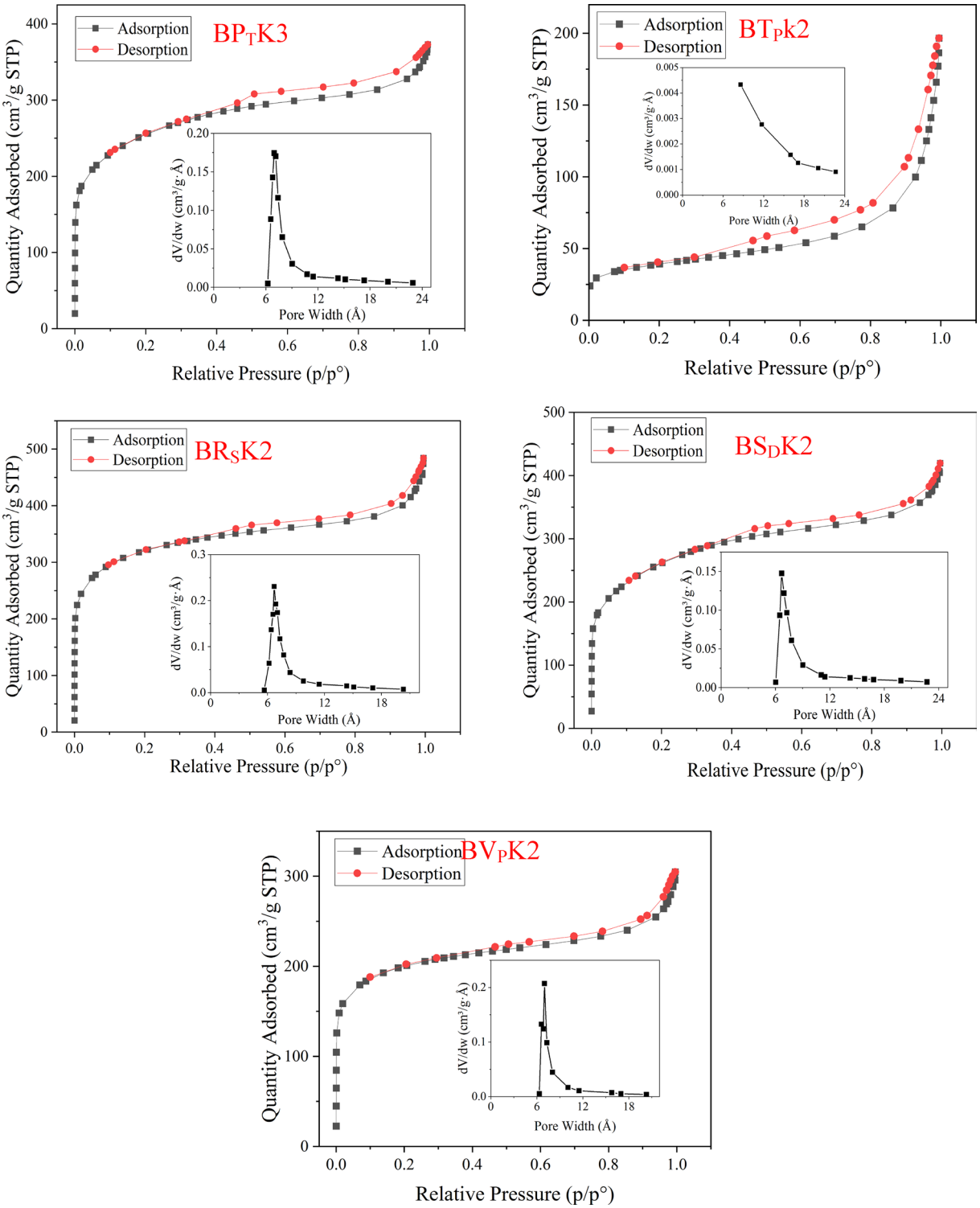

Fig. 4 BET results of adsorption and desorption behaviors of better-performed Morph-Genetic Porous Carbon (MGPC) produced from various wastes. Notes for optimal MGPC: BP_TK_2 (Palm tree pruning waste biochar, level 2 KOH), BT_Pk_2 (Tissue paper factory waste biochar, level 2 KOH), BR_SK_2 (Rice straw biochar, level 2 KOH), BS_DK_2 (Sawdust biochar, level 2 KOH), and BV_PK_2 (Vineyard pruning waste biochar, level 2 KOH)

environmental fields. In addition, more laboratory and field experiments are needed to evaluate how better-performing MGPCs behave in soil matrix in terms of improving soil compaction, preventing water loss, meeting plant water requirements, and affecting crop productivity. The findings of this study play a significant role in advancing global waste management policies, as they enable the conversion of agricultural and industrial wastes into highly valued biochar and MGPC. It is possible to recycle organic resources into a value-added by-product while reducing the volume of waste and mitigating environmental pollution. In summary, this research bridges the fields of materials science and environmental policy, advocating for waste management strategies that are ecologically sound, economically viable, and scientifically validated. This process helps achieve multiple sustainable development goals, maintains the quality of soil and water resources, and provides a scientific framework for sustainable waste management and improved agricultural productivity. Although more endeavors are needed to examine other game theory approaches, various types of porous materials, additional governing mechanisms, and even raw materials under different preparation conditions and scales are required to draw comprehensive conclusions.

Acknowledgements
This work is based upon research funded by the Iran National Science Foundation (INSF) under INSF-NSFC Joint Research Project No. 4021328. Dr. Mostafa Zabihi Silabi has also contributed to the running game-theoretic approach, whose valuable contributions are greatly appreciated.

Author Contributions
SHR SADEGHI: Conceptualization, Methodology, Investigation, Validation, Resources, Writing and Editing, Supervision, Project administration; S ZARE: Collection Data, Writing original draft preparation; S GHAREHMAHMUDLI: Conceptualization, Methodology, Writing original draft preparation, Investigation; H YOUNESI: Methodology, Reviewing and Editing; F Zhang: Writing-Review & Editing, Supervision, Projectadministration; M MIRZAHOSSEINI: CConceptualization, Methodology, Writing original draft preparation, Investigation; PS SADEGHI: Collection Data, Writing original draft preparation; M HOMAEE: Reviewing and Editing; Y PARVIZI: Reviewing and Editing; S NAN: Reviewing and Editing; Y Li: Reviewing and Editing.

Funding
This work is based upon research funded by the Iran National Science Foundation (INSF)under INSF-NSFC Joint Research Project No. 4021328.

Data availability
The datasets used or analyzed during the current study are available from the corresponding author upon reasonable request.

Declarations

Competing interests
The authors declare that they have no known competing financial interests or personal relationships that could have influenced the work reported in this paper.

Author details
[1]Department of Watershed Management Engineering, Faculty of Natural Resources, Tarbiat Modares University, 4641776489, Noor, Mazandaran Province, Iran. [2]Agrohydrology Research Group (Grant No. IG-39713), Tarbiat Modares University, Tehran 14115, Iran. [3]Department of Environmental Science, Faculty of Natural Resources, Tarbiat Modares University, Noor 46417-76489, Iran. [4]State Key Lab of Soil Erosion and Dryland Farming on the Loess Plateau, Institute of Soil and Water Conservation, Northwest A&F University, Shanghai, China. [5]Department of Soil Science, Tarbiat Modares University, Tehran 14115-336, Iran. [6]Soil Conservation and Watershed Management Research Institute, Agricultural Research, Education and Extension Organization (AREEO), Tehran, Iran. [7]Institute of Soil and Water Conservation, Northwest A&F University, Shanghai, China. [8]State Key Lab of Metal Matrix Composites, Shanghai Jiao Tong University, Shanghai 200240, China.

Received: 31 January 2025 Revised: 27 July 2025 Accepted: 1 September 2025
Published online: 02 March 2026

References

Adhami M, Sadeghi SHR, Duttmann R, Sheikhmohammady M (2020) Best soil co-management practices for two watersheds in Germany and Iran using game theory-based approaches. Sci Total Environ 698:134265
Al-Soudany K, Al-Gharbawi A, Al-Noori M (2018) Improvement of clayey soil characteristics by using activated carbon. MATEC Web Conf 162:01009
Amundson R, Berhe AA, Hopmans JW, Olson C, Sztein AE, Sparks DL (2015) Soil and human security in the 21st century. Annu Rev Environ Resour 40:75–98
Akhavan S, Jalalian A, Toomanian N, Honarjo N (2023) The application of multi-criteria decision-making model in land suitability assessment. Water and Soil 37(1):45–62
Avand M, Khiavi AN, Mohammadi M, Tiefenbacher JP (2023) Prioritizing sub-watersheds based on soil-erosion potential by integrating RUSLE and game-theory algorithms. Adv Space Res 72(2):471–487
Bahrami M, Amiri MJ, Beigzadeh B (2018) Adsorption of 2, 4-dichlorophenoxyacetic acid using rice husk biochar, granular activated carbon, and multi-walled carbon nanotubes in a fixed bed column system. Water Sci Technol 78(8):1812–1821
Bhagawan D, Poodari S, Chaitanya N, Ravi S, Rani YM, Himabindu V, Vidyavathi S (2017) Industrial solid waste landfill leachate treatment using electrocoagulation and biological methods. Desalin Water Treat 68:137–142
Black D (2025) Medical waste: risks and disposal strategies. Global Health J 22(4):78–88
Brown P et al (2024) Biochar as a climate-smart solution: A multi-criteria evaluation using the Condorcet method. J Environ Manag 23:215–230
Chen J, Wang X, Zhang Q (2023a) Game theory-based multi-criteria decision-making for environmental management. J Clean Prod 277:123–145
Chamberlin J, Jayne TS, Snapp S (2021) The role of active soil carbon in influencing the profitability of fertilizer use: empirical evidence from smallholder maize plots in Tanzania. Land Degrad Dev 32(9):2681–2694
Chen Z, Liu Y, Wang J (2023b) Cooperative game theory in Biochar selection for sustainable development. J Clean Prod 395:136852
FAO (2021)State of the World's Land and Water Resources for Food and Agriculture (SOLAW) 2022
Fard MM et al (2021) Biochar from agricultural waste: A review of preparation methods and applications. Renew Sustain Energy Rev 138:110594
Felsenthal DS, Machover M (1998) The measurement of voting power. edward elgar publishing. ISBN: 978–1858985910
Gehrlein WV, Fishburn PC (2023) Condorcet's paradox and the theory of voting. J Environ Sci Policy 45(3):12–19
Hemidat S, Achouri O, El Fels L, Elagroudy S, Hafidi M, Chaouki B (2022) Solid waste management in the context of a circular economy in the MENA region. Sustainability 14(1):480
Hewitt S, Ghogare R, Troxel W, Tenic E, Isaac D, Dhingra A (2023) Metatranscriptomic analysis of tomato rhizospheres reveals insight into plant-microbiome molecular response to biochar-amended organic soil. Fronti Analyt Sci 3:1205583

Khan MA, Salman AZ, Khan ST (2023) Indigenously produced biochar retains fertility in sandy soil through unique microbial diversity sustenance: a step toward the circular economy. Front Microbiol 14:1158784
Kim J, Park S, Choi H (2025) Porous biochar for heavy metal removal. Environ Sci Pollut Res Int 32:67–81
Kumar R, Singh P, Gupta A (2025a) Evolutionary game theory in sustainable biochar selection. Environ Sci Technol 59(1):112–123
Kumar S, Gupta R, Lee J (2025b) Thermal and chemical activation methods for the production of high-performance biochar. Renew Sustain Energy Rev 160:112349. https://doi.org/10.1016/j.rser.2025.112349
Kwiatkowski M, Broniek E (2020) An evaluation of the reliability of the results obtained by the LBET, QSDFT, BET, and DR methods for the analysis of the porous structure of activated carbons. Materials 13(18):3929
Lee D, Park S, Kim T (2022a) Non-cooperative game theory in biochar optimization: a Nash equilibrium approach. Renew Energy 186:274–285
Lee JH, Park MS, Kim HJ (2022b) Comparison of activation methods for biochar modification. J Clean Prod 340:130927
Lehmann J, Joseph S (2006) Biochar for environmental management: Science, technology, and implementation. Earthscan Publications 34:123–145
Li H, Chen Z, Yang T (2023a) Advanced applications of biochar in environmental management. Environ Sci Technol 57:102–118
Li H, Chen Z, Yang T (2025) Chemical activation of biochar for enhanced adsorption. Environ Technol Innov 30:45–58
Li Y, Zhang W, Wang Y (2023b) Biochar-derived porous carbons: synthesis and applications. Environ Res 231:115656
Martinez R et al (2025) Advances in biochar technology: A Condorcet method approach for assessing environmental benefits. Agricult Syst 34:67–78
Montanarella L, Panagos P, Ballabio C (2023) Soil erosion and its impact on global food security. Nat Sustain 6(3):215–225
Nasiri Khiavi A, Sadeghi SHR, Vafakhah M (2024) Comparative prioritization of sub-watersheds in flood generation using co-management best-worst method and game theory algorithm. Water Resour Manage. https://doi.org/10.1007/s11269-024-03873-1
Okoli OK (2016) Influence of chemical activation on the porous structure of carbon materials. J Environ Chem Eng 4(2):2030–2042
Park S, Kim H, Lee J, Chen Y (2025) Carbon nanotubes from biochar: a sustainable approach. Carbon 203:88–102
Patel MR, Panwar NL (2023) Biochar from agricultural crop residues: environmental, production, and life cycle assessment overview. Resour Conserv Recyc Advan 19:200173
Perea JD, Grima F (2021) Game theory for multi-criteria decision-making: a review of recent advances and applications. Eur J Oper Res 287(2):422–436
Pimentel D (2020) Soil erosion: a food and environmental threat. Environ Dev Sustain 2(4):111–123
Riker WH (2025) Hazardous Waste Management in Urban Areas. Indus Environ Res 30(1):34–47
Rouquerol J, Llewellyn PL, Sing KSW (1999) Adsorption by powders and porous solids: principles, methodology, and applications, 2nd ed
Roy B (1996) Multi-criteria Methodology for Decision Aiding. Kluwer Academic Publishers, New York, pp 45–68
Roy R, Chen J, Wang X (2023) Advanced methods in biochar production for industrial applications. Environ Res 230:115–132
Saaty TL (1980) The Analytic Hierarchy Process. McGraw-Hill, New York, pp 59–70
Sadeghi SHR, Ghavimi Panah MH, Younesi HA, Kheirfam H (2018) Ameliorating some quality properties of an erosion-prone soil using biochar produced from dairy wastewater sludge. CATENA 171:193–198
Sadeghi SHR, Hazbavi Z, Kiani Harchegani M (2016) Controllability of runoff and soil loss from small plots treated by biochar produced from vinasse. Sci Total Environ 541:483–490
Sadeghi SHR, Hazbavi Z, Kiani-Harchegani M, Younesi H, Sadeghi P, Angulo-Jaramillo R, Lassabatere L (2021) The hydrologic behavior of Loess and Marl soils in response to biochar and polyacrylamide mulching under laboratorial rainfall simulation conditions. J Hydrol 592:125620
Sadeghi SHR, Kiani-Harchegani M, Hazbavi Z, Sadeghi P, Angulo-Jaramillo R, Lassabatere L, Younesi H (2020) Field measurement of effects of individual and combined application of biochar and polyacrylamide on erosion variables in loess and marl soils. Sci Total Environ 728:138866
Sadeghi SHR, Silabi MZ, Vafakhah M (2024) Soil erosion-based sub-watershed prioritization through coupling various crop management and erosivity scenarios using game theory. Adv Space Res 73(12):5822–5835
Sharma S (2020) Effect of activation methods on the properties of porous carbon. J Energy Storage 32:101867
Sing KSW (1984) Reporting physisorption data for gas/solid systems. Pure Appl Chem 57(4):603–619
Singh KSW et al (2004) Physisorption of gases, with special reference to the determination of surface area and porosity. Pure Appl Chem 57(4):603–619
Smith A (2022) Recent advancements in biochar applications: A Condorcet ranking method for sustainability assessment. Environ Res 67:134–145
Smith T, Johnson P, Brown R (2025) Innovative waste management technologies for sustainable development. J Environ Sustain 45(2):123–135
Tang J, Zhu W, Kookana R (2021) Biochar properties and applications in sustainable agriculture and environmental management. Environ Sci Technol 55(2):1234–1245
Tideman TN (2006) Collective Decisions and Voting: The Potential for Public Choice. Ashgate Publishing. ISBN: 978–0754645979
Tideman TN (2023) Agricultural waste conversion: techniques and benefits. Int J Agric Sustain 18(2):56–64
Voukkali I, Papamichael I, Loizia P, Zorpas AA (2024) Urbanization and solid waste production: prospects and challenges. Environ Sci Pollut Res Int 31(12):17678–17689
Wang J, Zhang L, Chen X (2023) Synthesis and characterization of porous carbon materials for environmental and energy applications. J Mater Chem A 11(3):512–525
Wang X, Liu Y, Zhao M (2025a) Thermal processing of biochar for enhanced adsorption. Renew Mater J 48:78–89
Wang X, Liu Y, Zhao M (2025b) Thermal treatment of biochar for energy storage applications. J Carbon Res 68:102–115
Wang Z et al (2019) Carbon materials for CO_2 adsorption and energy storage. Renew Sustain Energy Rev 106:379–398
Wang Z, Zhao Y, Wang X, Li J (2018) Applications of mesoporous materials in gas separation. Chem Eng J 340:304–312
Zhang J, Li H (2020) An enhanced game-theoretical approach for multi-criteria decision-making problems in environmental management. J Clean Prod 268:122144
Zhang J, Zhao Y, Wu L (2024a) Hybrid AHP-game theory model for biochar feedstock selection. Sci Total Environ 905:167482
Zhang Y, Wang L, Li H (2024b) Optimization of porous carbon production via combined activation techniques. Carbon 201:842–859
Zhao X, Zhang Y, Li R, Wang J (2023) Recent advances in biochar materials for energy storage. Energy Storage Mater 56:121–135
Zhao Y, Wang X, Liu H, Chen Z, Li J (2020) Enhanced gas adsorption in mesoporous silica: a critical review. J Colloid Interface Sci 563:172–182
Zhou J, Dong Z, Yu Y, Sun Z, Zhou T, Chen Z (2025) Utilization of biochar derived from rice straw in petroleum bitumen: agricultural waste recycling and pavement sustainability. J Clean Prod. https://doi.org/10.1016/j.jclepro.2025.144808
Zhu H, An Q, Nasir ASM, Babin A, Saucedo SL, Vallenas A, Bi X (2023) Emerging applications of biochar: a review on techno-environmental-economic aspects. Bioresour Technol 388:129745
Zhu X, Wang Y, Li F, Chen Z, Zhang H (2018) Optimization of pore size distribution in mesoporous silica for efficient gas adsorption. Microporous Mesoporous Mater 265:314–324
Zohoori M, Ghani A (2017) Municipal solid waste management challenges and problems for cities in low-income and developing countries. Int J Sci Eng Appl 6(2):39–48